Uncertainty Quantification of Tissue Damage Due to Blood Velocity in Hyperthermia Cancer Treatments

Bruno Rocha Guedes[1], Marcelo Lobosco[1][0000−0002−7205−9509], Rodrigo Weber dos Santos[0000−0002−0633−1391], and Ruy Freitas Reis[1][0000−0001−5215−3744]

Departamento de Ciência da Computação
Universidade Federal de Juiz de Fora, Juiz de Fora, MG, BR
ruy.reis@ufjf.br

Abstract. In 2020, cancer was responsible for almost 10 million deaths around the world. There are many treatments to fight against it, such as chemotherapy, radiation therapy, immunotherapy, and stem cell transplant. Hyperthermia is a new treatment that is under study in clinical trials. The idea is to raise the tumour temperature to reach its necroses. Since this is a new treatment, some questions are open, which can be addressed via computational models. Bioheat porous media models have been used to simulate this treatment, but each work adopts distinct values for some parameters, such as the blood velocity, which may impact the results obtained. In this paper, we carefully perform an uncertainty quantification analysis due to the uncertainties associated with estimating blood velocity parameters. The results of the *in silico* experiments have shown that considering the uncertainties presented in blood velocity, it is possible to plan the hyperthermia treatment to ensure that the entire tumour site reaches the target temperature that kills it.

Keywords: Hyperthermia · Uncertainty Quantification · Porous Media · Mathematical Modeling · Computational Physiology

1 Introduction

According to the National Cancer Institute (NCI), in 2018, there were 18,1 million new cases of cancer registered and 9,5 million deaths worldwide caused by cancer [3]. As projected in early 2020 by a Brazilian non-governmental organisation, Oncoguia Institute, between 2020 and 2022 Brazil will register a total of 625,000 new cases of cancer per year. Considering all types of cancers, the most frequents in Brazil are non-melanoma skin cancer (177 thousand cases), breast and prostate cancer (66 thousand cases each), colon and rectum (41 thousand cases), lung (30 thousand cases), and stomach (21 thousand cases)[1]. According to the NCI, numerous treatments were created to treat cancer, for example, chemotherapy, radiation therapy, bone marrow transplant, and hyperthermia treatment [2].

ICCS Camera Ready Version 2021
To cite this paper please use the final published version:
DOI: 10.1007/978-3-030-77964-1_39

The hyperthermia treatment is considered a non-invasive method [16]. The basic idea of this technique is to increase the temperature of the target above a threshold aiming to destroy tumour cells. Besides, it is desired to minimise the damage to healthy tissue. Therefore, a consolidated technique to heat living tissues is based on the properties of magnetic nanoparticles. These particles produce heat when submitted to an alternating magnetic field through Néel relaxation and/or Brownian motion [17]. Due to biocompatibility, iron oxides Fe_3O_4 (magnetite) and $\gamma - Fe_2O_3$ (maghemite) are normally employed to hyperthermia treatment [18]. Furthermore, the nanoparticles can reach the target by the bloodstream or directly in the tumour site [16]. This study focuses on direct injection due to the facility to handle different tumour sizes and shapes.

In the context of this study, a mathematical model is employed to describe the behaviour of the tumour temperature over time due to hyperthermia treatment. Several models were developed and applied to describe the dynamics of heat in living tissues [14, 13, 21, 26, 25]. Among them, this work employed a porous media approach described in [14]. This model describes bioheat according to the properties of the living tissue such as density, specific heat, thermal conductivity, metabolism, blood temperature and velocity. Concerning blood velocity, the scientific literature describes that cancer growth can stimulate the angiogenesis of capillaries in the tumour site [9, 33]. Furthermore, it depends on the cancer type, stage, location and other specificities [12, 33]. So, this study chooses to describe the blood velocity as a density probability function based on the velocities found in the scientific literature intending to quantifying their influence on the bioheat dynamics.

To approach the employed mathematical model, this study uses an explicit strategy of the finite volume method (FVM) to obtain the numerical solution of the time-dependent partial differential equation [30, 6]. Moreover, the uncertainty quantification (UQ) technique was employed to quantify the blood velocity influence in the numerical output. UQ is a technique used to quantify uncertainties in real and computational systems. To incorporate the real variability and stochastic behaviour in systems, it is used statistical distributions as model inputs, with the goal validate and reduce the uncertainties of those parameters. Besisdes, UQ aims to quantify the influence of the variability in the parameter to the model output [29, 28, 32]

Several studies adopt the uncertainty quantification technique to propagate uncertainties of model parameters on both ordinary [4, 24, 22, 15, 23] and partial differential equations [31, 19, 5, 10, 20]. Concerning bioheat models, Fahrenholtz [7] employed generalised polynomial chaos to quantify the influence of model parameters of Pennes Bioheat model for planning MR-guided laser-induced thermal therapies (MRgLITT). Iero [11] also analyse the influence of uncertainties in hyperthermia treatment in patient-specific breast cancer using a modified version of Pennes model. In our study, we consider the propagation of the uncertainties related to the blood velocity in porous media and their impacts on a cancer hyperthermia treatment via magnetic nanoparticles.

ICCS Camera Ready Version 2021
To cite this paper please use the final published version:
DOI: 10.1007/978-3-030-77964-1_39

We organise this paper as follows. Section 2 describes the mathematical model and numerical techniques employed in this study. The results are presented in section 3 and discussed in section 4. Finally, section 5 presents the conclusions and plans for future work.

2 Material and Methods

In this study, the porous media equation is used in the representation of bioheat transference over the tumour cells [14, 25]. Uncertainties in the blood velocity in the tumour/healthy tissues were considered due to the study presented in [12] which calculates the velocity of the blood on tumour and healthy tissues. The values of this parameter are based on a uniform distribution, which randomly chooses a value in a given interval. The interval used for the blood velocity in tumour and healthy tissues was defined by the velocity presented in [12].

2.1 Mathematical Model

Let's consider that the modelled tissue containing the tumour is represented by an open bounded domain $\Omega \subset \mathbb{R}^2$ and $I \in (0, t_f] \subset \mathbb{R}^+$ is the simulated time. So, the bioheat model considering a medium porous approach can be defined as:

$$\begin{cases} \sigma \frac{\partial T}{\partial t} = \nabla \cdot \kappa \nabla T + \beta \frac{\rho_b u_b \varepsilon c_{pb}}{\delta} (T_b - T) + (1 - \varepsilon)(Q_m + Q_r), & \text{in } \Omega \times I, \\ \kappa \nabla T \cdot \vec{n} = 0, & \text{on } \partial\Omega \times I, \\ T(\cdot, 0) = 37, & \text{in } \Omega, \end{cases} \tag{1}$$

where $\sigma = [\rho c_p(1 - \varepsilon) + \rho_b c_{pb} \varepsilon]$, $\kappa = (1 - \epsilon)k_t + \epsilon k_b$. ρ, c_p and k_t are density, specific heat and thermal conductivity of the tissue, respectively. ρ_b, c_{pb}, k_b and u_b are density, specific heat, thermal conductivity and average velocity of the blood, respectively. ϵ, δ, β are porosity of the medium, average distance between the transverse blood vessels and a correction factor, respectively. T_b is the blood temperature. Q_m is the metabolic heat source, Q_r heat generated from the hyperthermia treatment, T_0 is the initial temperature, and the heat generated from hyperthermia treatment is given by:

$$Q_r(\vec{x}) = \sum_{i=1}^{n} A_i e^{-r\left(\vec{x}_i^2\right)/r_{0,i}^2}, \tag{2}$$

where n is the number of injections, A is maximum heat generation rate, $r\left(\vec{x}_i^2\right)$ is the distance from the injection point and r_0 is the radius of coverage of hyperthermia. The mathematical model of bioheat transference used was based on a previous study [25].

ICCS Camera Ready Version 2021
To cite this paper please use the final published version:
DOI: 10.1007/978-3-030-77964-1_39

2.2 Numerical Method

The finite volume method was employed to solve Eq. (1) [30]. The domain $\Omega \cup \partial\Omega$ is discretized into a set of nodal points defined by $S = \{(x_i, y_j); i = 0, .., N_x; j = 0, ..., N_y\}$ with N_x and N_y being the total number of points spaced with length Δx and Δy, respectively. Moreover, the time domain I is partitioned into N equal time intervals of length Δt, *i.e.* $t_n = n\Delta t$ for $n \in [0, N]$. Finally, the fluxes at the volumes surfaces for each nodal point were approximated by a central difference, and, to obtain an explicit method, the forward difference was employed for the time stepping. These numerical approaches ensure the first-order accuracy for time and a second-order for space. Thus, Eq. (1) is numerically computed by:

$$\begin{aligned} T_{i,j}^{n+1} = \frac{\Delta t}{\rho_c c_b \epsilon + \rho c (1-\epsilon)} \{ & \frac{[\kappa_{i+\frac{1}{2},j}(T_{i+1,j}^n - T_{i,j}^n) - \kappa_{i-\frac{1}{2},j}(T_{i,j}^n - T_{i-1,j}^n)]}{\Delta x^2} + \\ & \frac{[\kappa_{i,j+\frac{1}{2}}(T_{i,j+1}^n - T_{i,j}^n) - k_{i,j-\frac{1}{2}}(T_{i,j}^n - T_{i,j-1}^n)]}{\Delta y^2} \\ & + \beta_{i,j} \frac{p_b u_b \epsilon c_b}{\delta_{i,j}} (T_b - T) + (1-\epsilon)(Qm_{i,j} + Qr) \} + T_{i,j}^n \end{aligned} \tag{3}$$

where the thermal conductivity function is discontinuous, therefor the harmonic mean $\kappa_{i+\frac{1}{2},j} = \frac{2\kappa_{i,j}\kappa_{i+1,j}}{\kappa_{i,j}+\kappa_{i+1,j}}$ is adopted to ensure the flux continuity.

2.3 Uncertainty Quantification

In real-world, uncountable uncertainties are intrinsic to nature. In view of this, the uncertainty quantification (UQ) is employed for quantitative characterisation and uncertainties reduction on computational and real world applications, with the goal to determine how likely outcomes of models which uses stochastic behaviour. With the objective of including stochastic behaviour we employ UQ via Monte Carlo (MC) simulation [27]. The deterministic model described in Eq. (1) is solved several times considering the u_b parameter as a probability density function (PDF) to stochastic responses. MC draws samples of the u_b and evaluates the model for each of them. The results are used to provide statistical properties for the quantities of interest (QoI).

Consider that Y is the model solution for all space and time points. Furthermore, consider one or more uncertain input parameter Q and the known parameters K:

$$Y = f(x, y, t, Q, K). \tag{4}$$

Both Q and K are treated as sets of model parameters, and Y is computed using FVM described in the prior section. The uncertainty in this problem comes from the parameters in Q, which are assumed to have a known probability density function ϕ_Q. So, several samples are evaluated considering different values of Q

ICCS Camera Ready Version 2021
To cite this paper please use the final published version:
DOI: 10.1007/978-3-030-77964-1_39

according to ϕ_Q. Finally, the set of model results Y are used to evaluate the statistical properties of each QoI.

In this study, we perform the MC simulation aided by Chaospy library [8]. Chaospy is an open-source library designed to be used in the Python programming language, which provides functions for performing uncertainty quantification. Through this library, it is possible to create probabilistic distribution and samples variables to approach numerically the uncertainty quantification [8].

3 Results

This section presents the UQ analysis of temperature dynamics and tissue damage considering u_b as a PDF. To perform the UQ analysis we consider $10,000$ Monte Carlo iteration employing u_b as a uniform distribution. So, it was evaluated the mean and confidence interval (CI) in two different points on the domain, (one inside the tumour and another outside) over all time steps. Moreover, we present the mean of the final temperature distribution in the entire domain. Finally, it was estimated the amount of necrosis.

The values of parameters used in Eq. (1) to perform the Monte Carlo simulation are given by Table 1, where $X \sim F^{-1}(a, b)$ is a uniform distribution that generate a random value between a and b. The values of other parameters were based on a previous work [25].

Table 1. Model parameters values employed in Eq. (1).

Parameter	Description	Unit	Muscle	Tumour
c_p	Specific heat	(J/Kg^oC)	4200.0	4200.0
c_{pb}	Specific heat of blood	(J/Kg^oC)	4200.0	4200.0
k_t	Thermal conductivity of tissue	(W/m^oC)	0.51	0.56
k_b	Thermal conductivity of blood	(W/m^oC)	0.64	0.64
p	Density	(Kg/m)	1000.0	1000.0
p_b	Density of blood	(Kg/m)	1000.0	1000.0
u_b	Blood velocity	(mm/w)	$X \sim F^{-1}(1.5, 2.5)$	$X \sim F^{-1}(1.5, 4)$
δ	Average distance between blood vessels	(mm)	6.0	4.0
ϵ	porosity of the medium	-	0.02	0.02
β	Correction factor	-	0.1	0.1
Q_m	Metabolic heat source	W/m	420.0	4200.0

Two distinct scenarios were considered. The first one (Scenario 1) considers that magnetic nanoparticles are applied in a single point inside the tumour. The second scenario (Scenario 2) considers the application of magnetic nanoparticles in four distinct points. The domain is $x \in [0.0, 0.1]m$ and $y \in [0.0, 0.1]m$, with the tumour located in $(x, y) \in [0.04, 0.06] \times [0.04, 0.06]$.

ICCS Camera Ready Version 2021
To cite this paper please use the final published version:
DOI: 10.1007/978-3-030-77964-1_39

3.1 Scenario 1

In the first scenario, we consider only one injection site in the middle of the tumour, using the injection parameters given by Table 2.

Table 2. Parameters values for hyperthermia treatment with one injection site.

Position (m)	A	r_0
$(0.05, 0.05)$	$1.9 \times 10^6 W/m^3$	3.1×10^{-3}

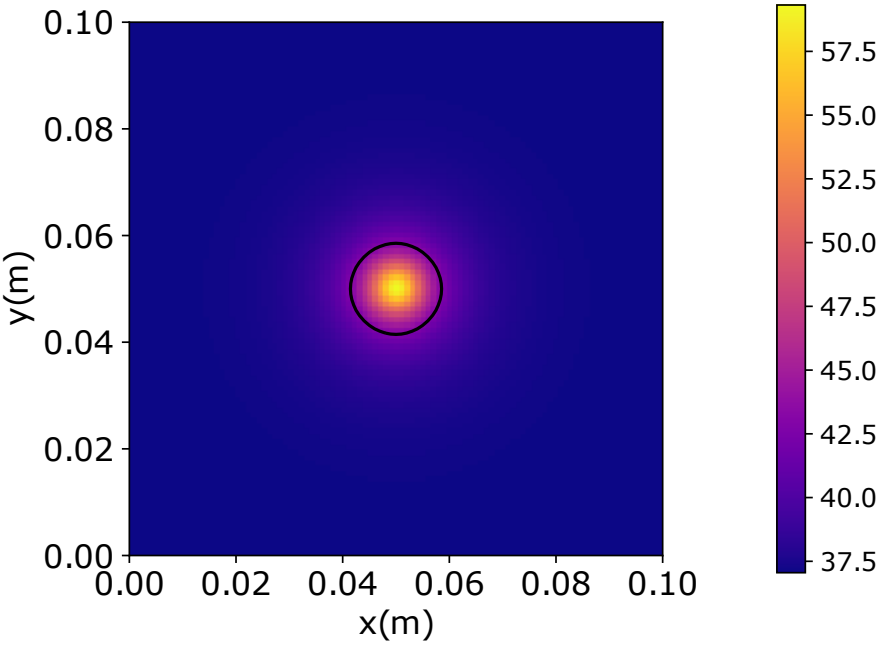

Fig. 1. Temperature distribution at $t = 5,000$s employing Eq. (3) with a tumour located in $(x, y) \in [0.04, 0.06] \times [0.04, 0.06]$ and one injection of nanoparticles as specified in Table 2. The solid black contour represents the temperature of 43^oC, highlighting the necrosis area.

The solution of Eq. (1) at $t = 5,000s$, using the method described by Eq. (3), is shown in Fig 2. This result shows the steady state temperature distribution. It is possible to observe an exponential decay in the temperature as the distance to the injection site increases.

ICCS Camera Ready Version 2021
To cite this paper please use the final published version:
DOI: 10.1007/978-3-030-77964-1_39

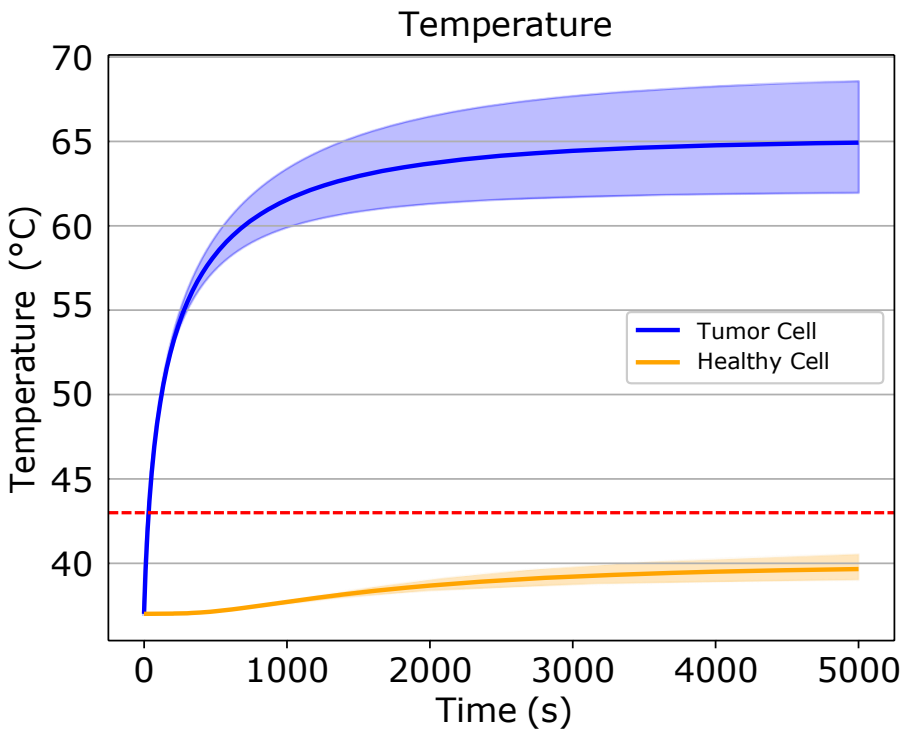

Fig. 2. Evolution of temperature determined by the Eq. (3) with one injection of nanoparticles located in the position presented in Table 2. The solid lines represents the mean temperature, shaded regions represents the 95% confidence interval and the red dashed line represents the temperature where the necroses occurs. The blue line and blue shaded represent the temperature of the tumour tissue located on the point $x = 0.05m$ and $y = 0.05m$. The orange line and orange shaded represent the temperature of a healthy tissue located on the point $x = 0.065m$ and $y = 0.065m$.

Fig. 2 presents the temperature evolution in both health and tumour tissues. For health tissue we consider the point seated in $(0.065m; 0.065m)$ and for tumour tissue a point located at $(0.05m; 0.05m)$. It can be observed that the temperature inside the tumour is much higher than 43^oC, which causes its necrosis, while the temperature on the health point does not reaches 43^oC.

Fig. 3A represents the evolution of tumour tissue necrosis over time. The percentage of tumour tissue killed due to the hyperthermia was computed considering all tumour points whose temperature was above 43^oC. This figure shows that up to 100% of the tumour is destroyed by the end of the simulation.

Fig. 3B represents the evolution of healthy tissue necrosis over time. This value was computed counting the number of healthy cell destroyed by a elevation of temperature above 43^oC. This figure shows that a small number of health tissue, 3.5%, were damaged due to the hyperthermia treatment.

ICCS Camera Ready Version 2021
To cite this paper please use the final published version:
DOI: 10.1007/978-3-030-77964-1_39

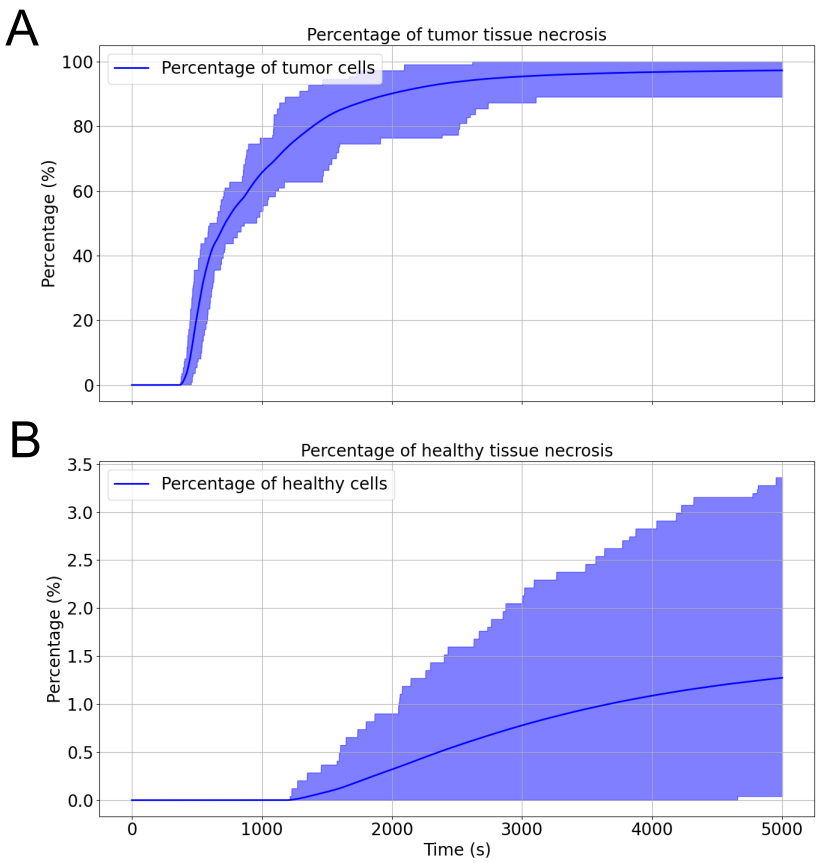

Fig. 3. (A) Percentage of tumour tissue killed by hyperthermia, and (B) Percentage of healthy tissue killed by hyperthermia. In both cases, one injection of nanoparticles was administered in the position given by Table 2. The percentage of tumour tissue killed by hyperthermia was computed at each time step considering all tumour cells whose temperature was above 43^oC. The solid line represents the mean and shaded regions represents the 95% confidence interval. The same method was applied to the healthy tissue.

3.2 Scenario 2

For the second scenario, we assume four injection sites in distinct positions. Table 3 presents the parameters values for this scenario.

The temperature distribution presented on Fig. 4 shows the solution of Eq. (3) on the final time step, *i.e.* $5,000$s.

Fig. 5 shows the evolution of temperature on a point inside the tumour (0.05m,0.05m) and one point outside it (0.065m,0.065m) in a simulation using four injection sites as described in Table 3. This figure shows that the tempera-

ICCS Camera Ready Version 2021
To cite this paper please use the final published version:
DOI: 10.1007/978-3-030-77964-1_39

Table 3. Parameters values for hyperthermia treatment with four injection sites.

Position (m)	A	r_0
$(0.045, 0.045)$	$0.425 \times 10^6 W/m^3$	3.1×10^{-3}
$(0.045, 0.055)$	$0.425 \times 10^6 W/m^3$	3.1×10^{-3}
$(0.055, 0.045)$	$0.425 \times 10^6 W/m^3$	3.1×10^{-3}
$(0.055, 0.055)$	$0.425 \times 10^6 W/m^3$	3.1×10^{-3}

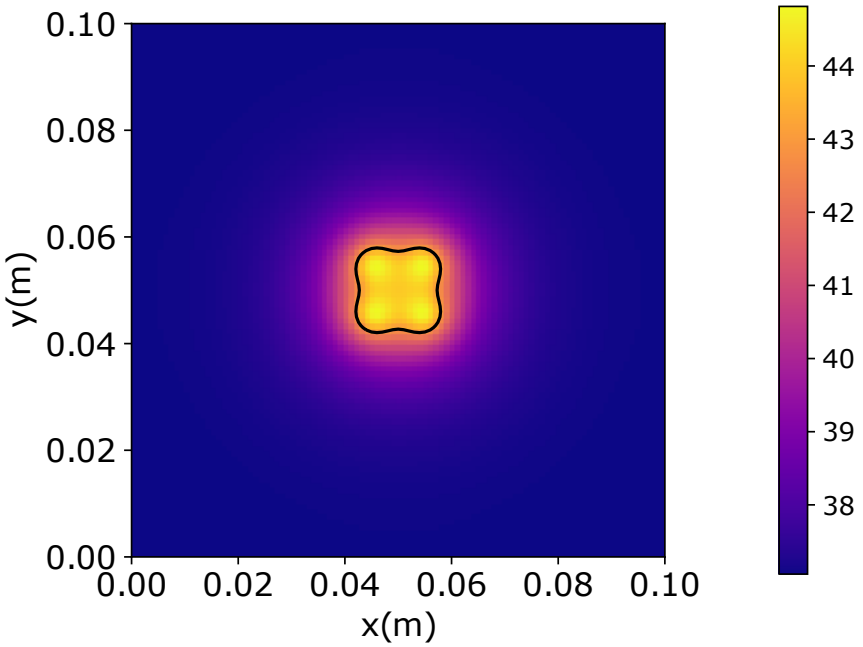

Fig. 4. Temperature distribution at $t = 5,000$s employing Eq. (3) with a tumour located in $(x, y) \in [0.04, 0.06] \times [0.04, 0.06]$ and four injections of nanoparticles as specified in Table 3. The solid black contour represents the temperature of 43^oC, highlighting the necrosis area.

ture inside the tumour rises above 43^oC, causing the tumour tissue to necrosis, while the temperature outside the tumour does not. Therefore, the healthy tissue located on the point outside the tumour does not reach 43^oC.

The percentage of tumour tissue killed due to hyperthermia with four injection site locations is shown in Fig. 6A. This result presents the percentage of tumour tissue killed over time, showing that at the end of the simulation, the expected value of tumour necrosis reaches 100%.

ICCS Camera Ready Version 2021
To cite this paper please use the final published version:
DOI: 10.1007/978-3-030-77964-1_39

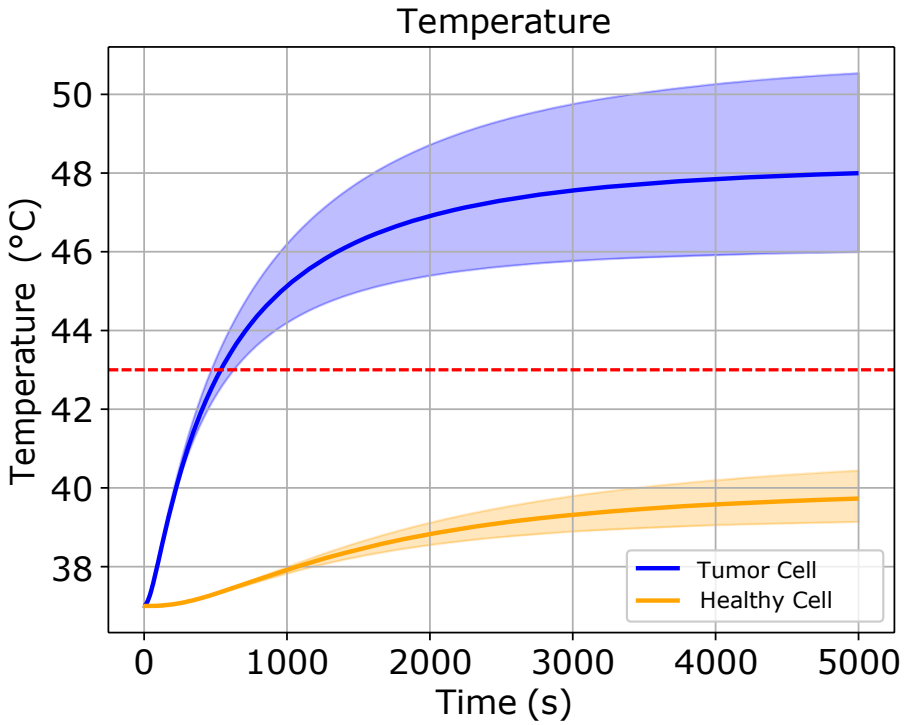

Fig. 5. Evolution of temperature determined by Eq. (3) with four injections of nanoparticles located in the positions presented in Table 3. The solid lines represents the mean temperature, shaded regions the 95% confidence interval and the red dashed line represents the temperature where the necroses occurs. The blue solid line and blue shaded represent a tumour tissue located at $x = 0.05m$ and $y = 0.05m$. The orange line and orange shaded represent a healthy tissue located at $x = 0.065m$ and $y = 0.065m$.

The consequences of hyperthermia treatment on healthy tissue are shown in Fig. 6B, which presents the percentage of healthy tissue killed due to the elevation of temperature above 43^oC. Only 3% of healthy tissue suffered necrosis at the end of the simulation of the hyperthermia treatment.

ICCS Camera Ready Version 2021
To cite this paper please use the final published version:
DOI: 10.1007/978-3-030-77964-1_39

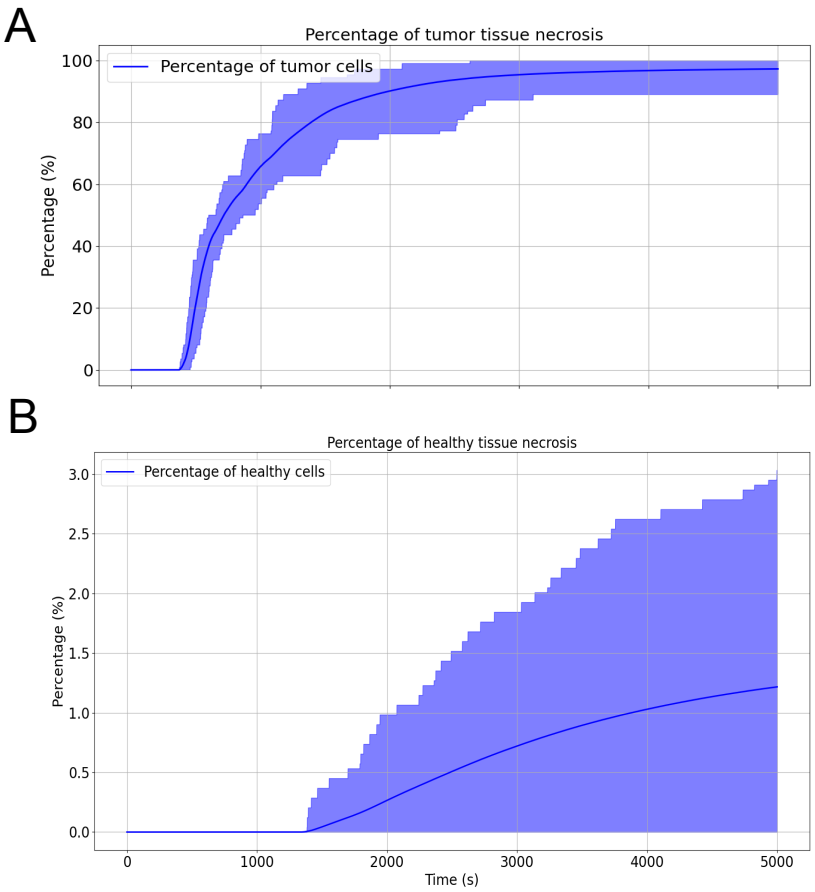

Fig. 6. (A) Percentage of tumour tissue killed by hyperthermia, and (B) Percentage of healthy tissue killed by hyperthermia. In both cases, four injection of nanoparticles was administered in the position given by Table 3. The percentage of tumour tissue killed by hyperthermia was computed at each time step considering all tumour cells whose temperature was above 43^oC. The solid line represents the mean and shaded regions represents the 95% confidence interval. The same method was applied to the healthy tissue.

4 Discussion

From the numerical results, it is possible to conclude that in both cases, with one and four injections sites on the tumour, the temperature rises above 43^oC at the tumour site which leads to its necrosis. Particularly Figs. 3A and 6A shows that the tumour is destroyed by the treatment. Comparing the different strategies for application points, one can observe that using one injection points leads to higher temperatures than four injection points. Besides, Figs. 3B and 6B

ICCS Camera Ready Version 2021
To cite this paper please use the final published version:
DOI: 10.1007/978-3-030-77964-1_39

show that using one injection point may cause around 0.5% more health tissue necrosis than four injection points.

5 Conclusions and Future Works

This work presents a two-dimensional simulation of hyperthermia cancer treatment in a heterogeneous tissue along with UQ analysis via MC. The simulation revealed that blood velocity influences the model outputs. Moreover, this study also demonstrates that the percentage of tumour necrosis is influenced by the variation of the blood velocity parameter. Also, this study shows that the percentage of healthy tissue damaged by the hyperthermia treatment is influenced by the uncertainties of the blood velocity parameter.

The results of simulations have shown that a hyperthermia treatment with four injections sites of nanoparticles on the tumour is more efficient, once the mean and CI of the tumour necrosis amount is higher than the case with only one injection. Besides, the results showed lower healthy tissue necrosis on the hyperthermia with four injections sites, in contrast with hyperthermia treatment with one injection site.

Furthermore, the simulation results show that the analysis of the uncertainties can provide important information for planning hyperthermia treatments. Additionally, this study demonstrates that uncertainty analysis can be an important tool for *in silico* medicine, mainly decreasing the need of clinical trial with animals as well as cohort studies with humans.

Although the goal of this paper is to analyse the blood velocity parameter from the mathematical model, it is possible to employ different types of probabilistic distribution, such as Normal distribution and LogNormal distribution. Further studies are needed to determine the best PDF to be employed to blood velocity. Different parameters can also be analyzed to determine their impact on the results of the mathematical model simulation. Furthermore, we intend to use real data from hyperthermia treatment and compare it with the *in silico* trials along with parameters of real patients to perform patient-specific experiments.

Acknowledgments

The authors would like to express their thanks to CAPES, CNPq, FAPEMIG and UFJF for funding this work.

References

1. Cancer estimates in brazil, http://www.oncoguia.org.br/conteudo/estimativas-no-brasil/1705/1/, last accesses on February 12 of 2020.
2. Comprehensive cancer information about treatments, https://www.cancer.gov/about-cancer/treatment/types, last accesses on February 12 of 2020.

ICCS Camera Ready Version 2021
To cite this paper please use the final published version:
DOI: 10.1007/978-3-030-77964-1_39

3. Comprehensive cancer information and statistics, https://www.cancer.gov/about-cancer/understanding/statistics, last accesses on February 12 of 2020.
4. Bhaumik, P., Ghosal, S.: Efficient Bayesian estimation and uncertainty quantification in ordinary differential equation models. Bernoulli **23**(4B), 3537 – 3570 (2017). https://doi.org/10.3150/16-BEJ856, https://doi.org/10.3150/16-BEJ856
5. Campos, J.O., Sundnes, J., Dos Santos, R.W., Rocha, B.M.: Effects of left ventricle wall thickness uncertainties on cardiac mechanics. Biomechanics and modeling in mechanobiology **18**(5), 1415–1427 (2019)
6. Eymard, R., Gallouët, T., Herbin, R.: Finite volume methods. Handbook of numerical analysis **7**, 713–1018 (2000)
7. Fahrenholtz, S.J., Stafford, R.J., Maier, F., Hazle, J.D., Fuentes, D.: Generalised polynomial chaos-based uncertainty quantification for planning mrglitt procedures. International Journal of Hyperthermia **29**(4), 324–335 (2013)
8. Feinberg, J., Langtangen, H.P.: Chaospy: An open source tool for designing methods of uncertainty quantification. Journal of Computational Science **11**, 46–57 (2015)
9. Hicklin, D.J., Ellis, L.M.: Role of the vascular endothelial growth factor pathway in tumor growth and angiogenesis. Journal of clinical oncology **23**(5), 1011–1027 (2005)
10. Hurtado, D.E., Castro, S., Madrid, P.: Uncertainty quantification of 2 models of cardiac electromechanics. International journal for numerical methods in biomedical engineering **33**(12), e2894 (2017)
11. Iero, D.A.M., Crocco, L., Isernia, T.: Thermal and microwave constrained focusing for patient-specific breast cancer hyperthermia: A robustness assessment. IEEE Transactions on Antennas and Propagation **62**(2), 814–821 (2014). https://doi.org/10.1109/TAP.2013.2293336
12. Ishida, H., Hachiga, T., Andoh, T., Akiguchi, S.: In-vivo visualization of melanoma tumor microvessels and blood flow velocity changes accompanying tumor growth. Journal of Applied Physics **112**(10), 104703 (2012)
13. Jiji, L.M.: Heat transfer in living tissue. In: Heat Conduction, pp. 302–346. Springer (2009)
14. Khaled, A.R., Vafai, K.: The role of porous media in modeling flow and heat transfer in biological tissues. International Journal of Heat and Mass Transfer **46**(26), 4989–5003 (2003)
15. d. L. e Silva, L., Xavier, M.P., dos Santos, R.W., Lobosco, M., Reis, R.F.: Uncertain quantification of immunological memory to yellow fever virus. In: 2020 IEEE International Conference on Bioinformatics and Biomedicine (BIBM). pp. 1281–1288 (2020). https://doi.org/10.1109/BIBM49941.2020.9313282
16. Minkowycz, W., Sparrow, E.M., Abraham, J.P.: Nanoparticle heat transfer and fluid flow, vol. 4. CRC press (2012)
17. Moros, E.: Physics of thermal therapy: fundamentals and clinical applications. CRC Press (2012)
18. Moroz, P., Jones, S., Gray, B.: Magnetically mediated hyperthermia: current status and future directions. International Journal of Hyperthermia **18**(4), 267–284 (2002)
19. Nardini, J.T., Bortz, D.: The influence of numerical error on parameter estimation and uncertainty quantification for advective pde models. Inverse Problems **35**(6), 065003 (2019)
20. Osnes, H., Sundnes, J.: Uncertainty analysis of ventricular mechanics using the probabilistic collocation method. IEEE transactions on biomedical engineering **59**(8), 2171–2179 (2012)

ICCS Camera Ready Version 2021
To cite this paper please use the final published version:
DOI: 10.1007/978-3-030-77964-1_39

21. Pennes, H.H.: Analysis of tissue and arterial blood temperatures in the resting human forearm. Journal of applied physiology **1**(2), 93–122 (1948)
22. Reagan, M.T., 4, H.N.N., Debusschere, B.J., Maître, O.P.L., Knio, O.M., Ghanem, R.G.: Spectral stochastic uncertainty quantification in chemical systems. Combustion Theory and Modelling **8**(3), 607–632 (2004). https://doi.org/10.1088/1364-7830/8/3/010
23. Reis, R.F., de Melo Quintela, B., de Oliveira Campos, J., Gomes, J.M., Rocha, B.M., Lobosco, M., Weber dos Santos, R.: Characterization of the covid-19 pandemic and the impact of uncertainties, mitigation strategies, and underreporting of cases in south korea, italy, and brazil. Chaos, Solitons & Fractals **136**, 109888 (2020). https://doi.org/https://doi.org/10.1016/j.chaos.2020.109888, https://www.sciencedirect.com/science/article/pii/S0960077920302885
24. Reis, R.F., Oliveira, R.S., Quintela, B.d.M., Campos, J.d.O., Gomes, J.M., Rocha, B.M., Lobosco, M., dos Santos, R.W.: The quixotic task of forecasting peaks of covid-19: Rather focus on forward and backward projections. Frontiers in Public Health **9**, 168 (2021). https://doi.org/10.3389/fpubh.2021.623521, https://www.frontiersin.org/article/10.3389/fpubh.2021.623521
25. Reis, R.F., dos Santos Loureiro, F., Lobosco, M.: Parameters analysis of a porous medium model for treatment with hyperthermia using openmp. In: Journal of Physics: Conference Series. vol. 633, p. 012087. IOP Publishing (2015)
26. Reis, R.F., dos Santos Loureiro, F., Lobosco, M.: 3d numerical simulations on gpus of hyperthermia with nanoparticles by a nonlinear bioheat model. Journal of Computational and Applied Mathematics **295**, 35–47 (2016)
27. Rubinstein, R.Y., Kroese, D.P.: Simulation and the Monte Carlo method, vol. 10. John Wiley & Sons (2016)
28. Saltelli, A., Ratto, M., Andres, T., Campolongo, F., Cariboni, J., Gatelli, D., Saisana, M., Tarantola, S.: Global sensitivity analysis: the primer. John Wiley & Sons (2008)
29. Sullivan, T.J.: Introduction to uncertainty quantification, vol. 63. Springer (2015)
30. Versteeg, H.K., Malalasekera, W.: An introduction to computational fluid dynamics: the finite volume method. Pearson education (2007)
31. Wu, J.L., Michelén-Ströfer, C., Xiao, H.: Physics-informed covariance kernel for model-form uncertainty quantification with application to turbulent flows. Computers & Fluids **193**, 104292 (2019)
32. Xiu, D.: Numerical methods for stochastic computations: a spectral method approach. Princeton university press (2010)
33. Zhou, W., Chen, Z., Zhou, Q., Xing, D.: Optical biopsy of melanoma and basal cell carcinoma progression by noncontact photoacoustic and optical coherence tomography: In vivo multi-parametric characterizing tumor microenvironment. IEEE transactions on medical imaging **39**(6), 1967–1974 (2019)

ICCS Camera Ready Version 2021
To cite this paper please use the final published version:
DOI: 10.1007/978-3-030-77964-1_39